Particle identification at the EIC with a modular imaging Cherenkov counter.

J. Matthew Durham, Hubert W. van Hecke, Jin Huang, Ming X. Liu
Los Alamos National Laboratory, Los Alamos, NM 87545, USA

December 2, 2013

Abstract

We present a proposal for a modular particle identification device capable of identifying charged pions, kaons, and protons at the proposed electron-ion collider.

1 Introduction

Detectors at the EIC need a wide range of capabilities in order to achieve the proposed physics goals. Particle identification is one of these. The EIC White Paper [2] refers (some of) to these requirement as follows:

"... the momentum range of pions in the central detector region ($-1 < \eta < 1$) of typically 0.3 GeV/c to 4 GeV/c with a maximum of about 10 GeV/c. A combination of high resolution time-of-flight (ToF) detectors (with timing resolutions Δt $\sim$ 10ps), a DIRC or a proximity focusing Aerogel RICH may be considered for particle identification in this region. Hadrons with higher momenta go typically in the forward (ion) direction for low lepton beam energies, and in the backward direction for higher lepton beam energies. The most viable detector technology for this region of the detector is a Ring-Imaging Cherenkov (RICH) detector with dual-radiators."

This research proposal aims to lead to the development of a modular imaging Cherenkov counter that can fulfill the requirements outlined in the White Paper.

2 Detector Design

2.1 Detector Concept

A schematic diagram of an imaging Cherenkov detector is shown in Fig. 1. A Cherenkov radiator of thickness t is followed at a distance d by an

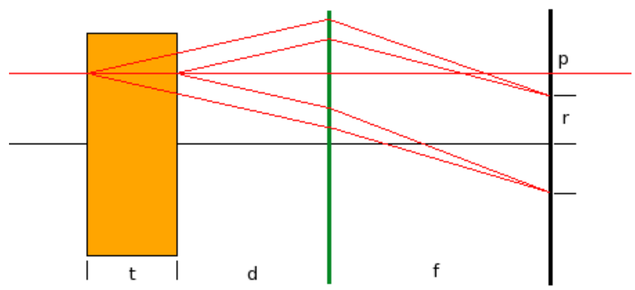

Figure 1: A diagram of an generic imaging Cherenkov counter: a radiator of thickness t, followed by an imaging element (green) of focal length f, and a photon detector (black).

optical imaging element, typically a mirror or a lens, and an imaging plane at distance f from the imaging element. A Cherenkov ring with radius r is formed in the image plane, where a photon detector registers the Cherenkov light. This detector may also register the passage of the charged particle at p. The image in the focal plane is independent of d, and we set this distance to zero. The ring radius r is determined by the Cherenkov angle θ and by the focal length f of the imaging element: $r = f * tan(\theta)$. Fig. 2 shows the radiator, imaging elements, which is taken to be a lens, and the photon detector plane, all enclosed in a box. Under certain conditions, namely when incident particle paths make an angle with the horizontal greater than the Cherenkov angle, or when the incident particle is very close to the boundary, some of the photons will hit the box wall. If the inside surfaces of the box are made of flat mirror material, these photons will not be lost. The pattern formed in the image plane may be distorted as in Fig. 3, but these are shapes that can be recognized by the pattern recognition software.

Fig. 4 shows the how several units can be arranged into a projective geometry to form a relatively shallow, self-contained wall. In such an arrangement, high-momentum particles will be approximately normally incident on each

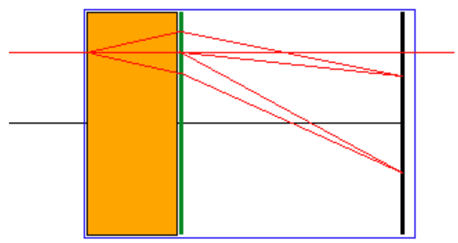

Figure 2: The imaging element is placed against the exit surface of the radiator, and all elements are enclosed in a box with mirror surfaces.

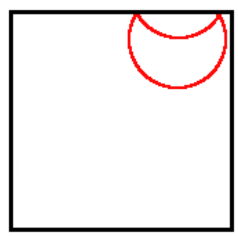

Figure 3: If an incident particle makes a large angle wrt the optical axis, the Cherenkov ring in the image plane may become folded.

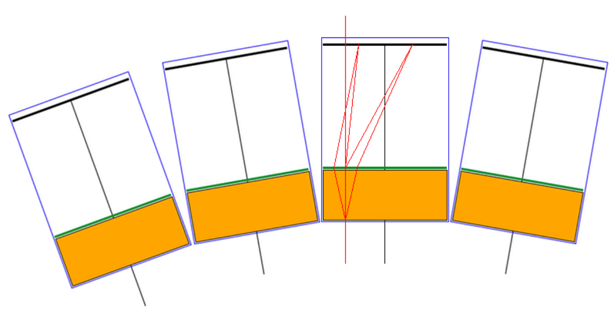

Figure 4: Individual units may be stacked to make a hermetic, projective detector wall.

device, and the Cherenkov rings will all be centered on the optical axes. Depending on the choice of the focal length f of the lens, the photon detector does not need to extend all the way to the edge of the device - it only needs to cover the area where rings of interest are projected.

Note that although the proposed design is for a modular imaging device, other types of Cherenkov detectors can be derived from this concept. For example, omitting the lens would would turn this into a proximity-focusing unit, and omitting pixelation of the detector plane would result in a threshold Cherenkov counter.

2.2 Radiator choice

If we want to distinguish Kaons from pions in the few-GeV range, the refractive index n of the Cherenkov radiator needs to be in the 1.01-1.02 range as can be seen in Fig. 5, and the only material with such indices is silica

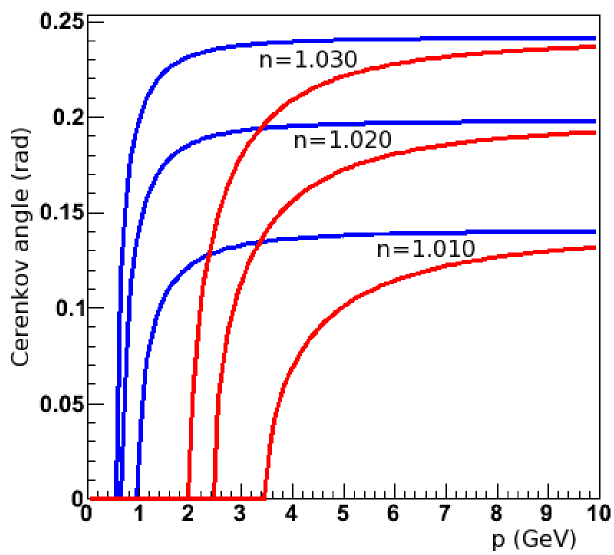

Figure 5: Threshold curves for Kaons (red) and pions (blue) for different refractive indices.

aerogel. Fig. 6 shows a Cherenkov ring produced using a 450 GeV proton beam [4, 5]. The outer ring is formed by Cherenkov radiation from aerogel with refractive index n=1.010, and the small ring in the center results from Cherenkov radiation from air in the detector. Photons in aerogel are subject

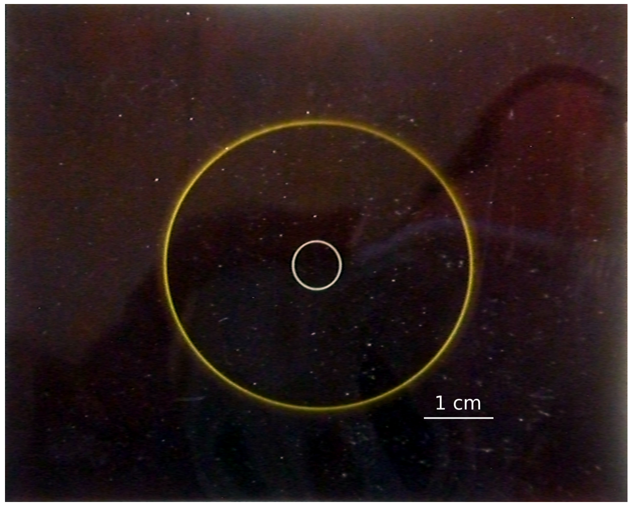

Figure 6: Cherenkov rings produced by a 450 GeV/c proton beam traversing an aerogel sample with refractive index n=1.010. The small central ring is from Cherenkov radiation in air.

to Rayleigh scattering, which scales as λ^{-4}, where λ is the wavelength. Fig. 7 shows a transmission spectrum of a 3 cm thick sample of aerogel (histogram). The transmission spectrum can be parametrized by

$$T = Ae^{-Ct/\lambda^4}$$

where A is the transmission at large wavelengths, t is the sample thickness and C (for 'clarity') is a measure of the quality of the sample - the lower C, the more photons exit unscattered.

Photons in the focal-plane Cherenkov ring are those that are not scattered before exiting the aerogel. This favors photons at long wavelengths, and photons produced close to the exit surface of the radiator. Fig. 8 shows in the left panel a typical spectrum of produced Cherenkov photons, falling with λ^{-2}. In the right panel are shown the spectra of scattered and unscattered photons for aerogel of different values of the clarity C. The distributions of unscattered photons have a broad maximum at wavelengths in the 300-500 nm range, and their number increases with decreasing values of C.

Current state-of-the-art aerogel with refractive indices in the range of interest can be produced with values of C as low as 60 $10^{-4} \mu m^4/cm$.

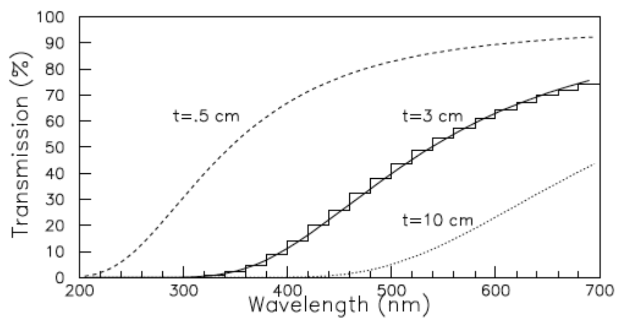

Figure 7: Transmission spectrum (histogram) of a 3cm sample of aerogel. Also shown are a fit to the spectrum, and spectra corresponding to transmission through 0.5 and 10 cm of the same material, derived from the fit.

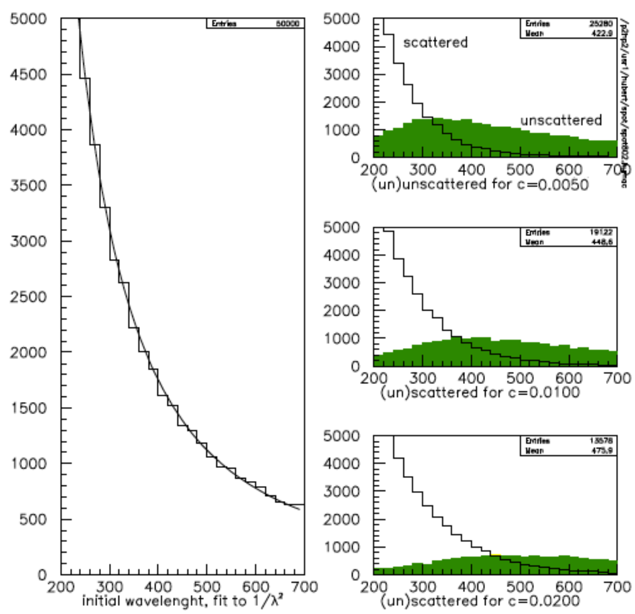

Figure 8: Left: spectrum of produced Cherenkov photons. Right: spectra of scattered (histogram) / unscattered (green) photons, for different values of the aerogel parameter C.

2.2.1 Aerogel availability

Worldwide, a very small number of facilities are capable of producing aerogel with the properties required for use in Cherenkov detectors. Companies or institutions that have supplied aerogel for such detectors in the past include

- Budker Institute for Nuclear Physics, Novosibirsk
- KEK, Japan
- Matsushita Electric Works, Japan
- Airglass AB, Sweden

Current availability of suitable aerogel is being explored.

2.3 The Imaging Element

In most imaging Cherenkov detectors currently in use, the element that images the Cherenkov photons into a sharp ring is a concave mirror, or a set of mirrors. In such cases the detector plane may need to be placed to the sides of the radiator volume, which makes hermetic, modular construction impossible.

In this proposal, the imaging element is an (acrylic) Fresnel lens. These typically are 1 mm thick or less. A transmission spectrum of such a lens is shown in Fig. 9b. This lens would absorb most of the scattered photons, which would otherwise contribute to a diffuse background in the detector plane, and it would pass most of the unscattered photons. Cherenkov light is emitted at angles θ where

$$cos(\theta) = \frac{1}{\beta n}$$

If we assume that n does not vary appreciably with wavelength, then the number of photons produced per unit path length is given by

$$dN/dx = 2\pi\alpha sin^2\theta \left\{ \frac{1}{\lambda_1} - \frac{1}{\lambda_2} \right\}$$

where α is the fine structure constant. For a typical Cherenkov angle of 10°, and a wavelength interval $[\lambda_1, \lambda_2]$ of 300-500 nm, we can expect about 14 produced photons/cm.

Because of the properties of the aerogel and the acrylic, the photon detector in the focal plane should be sensitive in the 300-500 nm range.

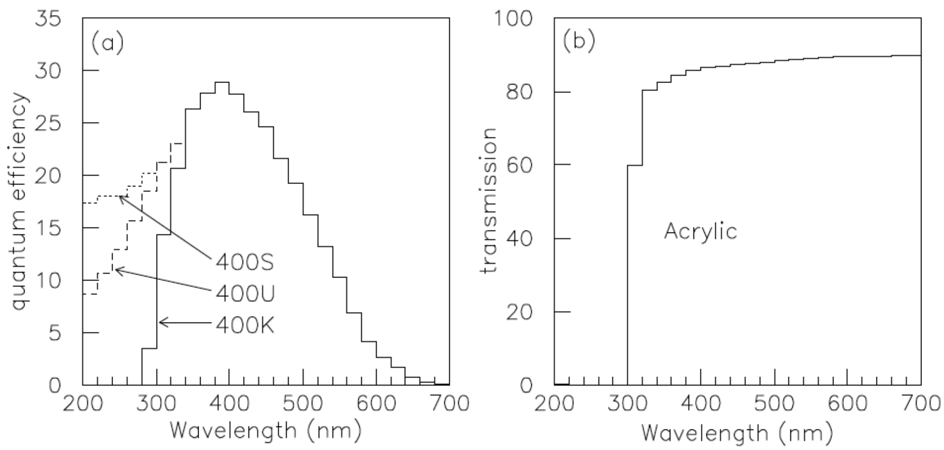

Figure 9: Left: Quantum efficiency of the EMI9125 PMT with selected photocathodes (a), and transmission spectrum of a UV-acrylic fresnel lens.

2.4 The Photon Detector

The requirements for the photon detector will have to be refined with MC studies. In particular, the required minimum pixelization depends on the

The wavelength range of interest for Cherenkov photons produced in the aerogel radiator will be 300-500 nm, which is in the near-UV to green portion of the spectrum. A variety of photon detection technologies exist which are senstive in this range, each of which have their own merits and deficits, as discussed in the following sections.

The detection plane needs to be sensitive in the visible portion of the electromagnetic spectrum, an it needs to be sufficiently pixelated so that ring diameters and positions can be determined. In the context of the proposed device, several photon detection methods can be invstigated.

2.4.1 PMTs - PhotoMultiplier Tubes

This is a tried-and-true technology, and is successfully used in the LHCb imaging aerogel Cherenkov counter. However, as the total sensor area in one module is of scale 10-20 cm square, plain PMTs are too large for this application. However, new pixelated designs look promising, such as the Hamamatsu H8500 tubes, which are 5x5 cm, with 8x8 pixels and a high packing fraction.

Additionally, PMT function suffers in the presence of a magnetic field, which would limit the usefulness of the modular design concept. The relativeley high materials budget of PMTs could also introduce undesirable backgrounds. While PMTs could be mounted outside the acceptance to detect Cherenkov photons reflected from mirrors, this greatly complicates the design and, again, limits the universality of the detector.

2.4.2 APDs - Avalanche PhotoDiodes

APDs are small (typically 1 mm^2 active area) and have a relatively high quantum efficiency of 40% in the wavelength range of interest. They could provide the necessary pixellation to resolve differences in ring radii for different particle species. To minimize channel count, an array of non-contiguous APDs could be built, with a matching array of Winston-like cones in front. The cone shape could be optimized for the range of incident photon angles at each coordinate. Such a cone array can be fabricated on a 3D printer. The largest drawback of APD technology is currently the cost. $Givesomeestimateof APDcostperchannelhere.$

2.4.3 LAPPDs - Large Area Picosecond Photo-Detectors

LAPPDs [1] are based on image-intensifier micro-channel plate technology. Though fast timing is not required for the proposed application, LAPPDs are large-area (up to 20x20 cm) photon detectors with sensitivity at visible wavelengths, possibly suitable for the proposed application. However, to date this technology has not been proven on a scale that is suitable for this application.

2.4.4 GEMs - Gas Electron Multipliers

GEMs with a reflective photocathode film deposited on the uppermost surface have recently emerged as an attractive photon detection technology (cite HBD paper and others). Since the amplification structure is effectively decoupled from the charge collection plane, the geometry of the readout pattern can be optimized for the desired resolution with a minimal channel count. GEMs are available in various sizes from a range of US and foreign manufacturers, and function well in magnetic fields. They have also been shown to operate in a variety of gases that are transparent in the wavelength range of interest, which minimizes Cherenkov photon losses.

In the wavelength range of interest for Cherenkov photons produced in aerogel, ~300-500 nm, bialkali crystals such as Sb-Cs-K have the necessary quantum efficiency (QE) to function as photocathodes (insert figure). Early studies by Breskin et al. [3] have shown a reasonable QE when deposited onto GEM foils. However, the effective QE is also heavily dependent on the choice of gas, which effects photoelectron backsacttering into the photocathode.

Part of this research will therefore be to find the appropriate gas or mixture of gases to maximize the collected photoelectron yield in the visible range. Bialkali photocathodes are notoriously reactive with oxygen, and therefore the detector must be assembled without exposure to oxygen. However, the relatively small size and modular nature of the design considerably simplifies this task. In addition, the design of the detector greatly simplifies maintenance during operation and allows for straightforward replacement of individual modules, if necessary.

The primary technology to be persued in this project is visible-light sensitive GEMs.

3 Capabilities

In order to carry out the proposed research, equipment, technologies and expertise will be needed that may not available in our research team. These include equipment vapor deposition, optical measurements, characterization of surfaces and the like. However, all such capabilities are available at Los Alamos National Lab, and we plan to make full use of them.

4 Request for Funds

Budgetary information.

References

[1] The large area picosecond photo-detectors project.

[2] A Accardi et al. Electron ion collider: The next qcd frontier. *arXiv 1212.1701*, 2012.

[3] Breskin et al. breskin paper title. 1994.

[4] D.E. Fields et al. Use of aerogel for imaging cherenkov counters. *NIM*, A349:431–437, 1994.

[5] H. van Hecke. A spot-imaging cerenkov counter. *NIM*, A343:311–315, 1994.